

QCD bounds on leading-order hadronic vacuum polarization contributions to the muon anomalous magnetic moment

Siyuan Li^{*1}, T.G. Steele^{†1}, J. Ho^{‡2}, R. Raza^{§3}, K. Williams^{¶3}, and R.T. Kleiv^{||3}

¹Department of Physics and Engineering Physics, University of Saskatchewan,
Saskatoon, SK, S7N 5E2, Canada

²Department of Physics, Dordt University, Sioux Center, Iowa, 51250, USA

³Department of Physics, Thompson Rivers University, Kamloops, BC, V2C 0C8,
Canada

August 1, 2024

Abstract

QCD bounds on the leading-order (LO) hadronic vacuum polarization (HVP) contribution to the anomalous magnetic moment of the muon ($a_\mu^{\text{HVP,LO}}$, $a_\mu = (g - 2)_\mu / 2$) are determined by imposing Hölder inequalities and related inequality constraints on systems of Finite-Energy QCD sum-rules. This novel methodology is complementary to lattice QCD and data-driven approaches to determining $a_\mu^{\text{HVP,LO}}$. For the light-quark (u, d, s) contributions up to five-loop order in perturbation theory in the chiral limit, LO in light-quark mass corrections, next-to-leading order in dimension-four QCD condensates, and to LO in dimension-six QCD condensates, we find that $(657.0 \pm 34.8) \times 10^{-10} \leq a_\mu^{\text{HVP,LO}} \leq (788.4 \pm 41.8) \times 10^{-10}$, bridging the range between lattice QCD and data-driven values.

^{*}siyuan.li@usask.ca

[†]tom.steele@usask.ca

[‡]jason.ho@dordt.edu

[§]rraza@tru.ca

[¶]williamsk16@mytru.ca

^{||}rkleiv@tru.ca

1 Introduction

In the summer of 2023, the Muon $g - 2$ experiment at Fermilab announced an updated result to the measurement of $a_\mu \equiv (g - 2)_\mu/2$, increasing the precision of their previous measurement by a factor of two [1] (see also *e.g.*, Ref. [2]). This updated experimental result reinforces the tension between experimental measurements and predictions from the Standard Model using data-driven and dispersive methods, pushing the disagreement between this new experimental observation and the prediction from theory [3] up to 5.0σ [1]. In addition to this new experimental evidence, recent precision measurements of the pion form factor by CMD-3 have been used to calculate the lowest-order hadronic contributions to a_μ [4], and found agreement with [1] to within 0.9σ . Furthermore, a recent calculation by the Budapest–Marseille–Wuppertal (BMW) collaboration using lattice QCD (LQCD) reached sub-percent levels of precision competitive with data-driven and dispersive methods [5]. This high-precision LQCD calculation of a_μ is in significantly better agreement with current experimental measurements. While efforts are ongoing by the LQCD community to produce new calculations of sub-percent precision [6], the results of the BMW collaboration produced a new tension between theoretical methods.

Currently, contributions to a_μ from the hadronic vacuum polarization (HVP) dominate the uncertainties in the Standard Model calculation. In the data-driven approach, the leading-order (LO) dispersion integral for the contributions to a_μ from HVP (*i.e.*, $a_\mu^{\text{HVP,LO}}$) is given by [3, 7, 8]

$$a_\mu^{\text{HVP,LO}} = \frac{1}{4\pi^3} \int_{4m_\pi^2}^{\infty} \sigma^H(t) K(t) dt \quad (1)$$

where σ^H is the e^+e^- to hadrons cross section and $K(t)$, the kernel function, is given by

$$K(t) = \int_0^1 dx \frac{x^2(1-x)}{x^2 + (1-x)t/m_\mu^2}, \quad (2)$$

where m_μ is the muon mass. Using the hadronic R -ratio

$$R(t) = \frac{\sigma^H(t)}{\sigma(e^+e^- \rightarrow \mu^+\mu^-)}, \quad (3)$$

with

$$\sigma(e^+e^- \rightarrow \mu^+\mu^-) = \frac{4\pi\alpha^2}{3t^2} (t + 2m_\mu^2) \sqrt{1 - \frac{4m_\mu^2}{t}} = \frac{4\pi\alpha^2}{3t} + \mathcal{O}\left(\frac{1}{t^3}\right), \quad (4)$$

where α is the fine-structure constant, Eq. (1) can be expressed as

$$a_\mu^{\text{HVP,LO}} = \frac{\alpha^2}{3\pi^2} \int_{4m_\pi^2}^{\infty} \frac{1}{t} R(t) K(t) dt, \quad (5)$$

where the approximation associated with (4) is negligible. Since the hadronic R -ratio can be expressed in terms of the hadronic vacuum polarization spectral function $R(t) = 12\pi\text{Im}\Pi^H(t)$ [8, 9], a QCD expression for Eq. (1) can be written in terms of the hadronic spectral function $\text{Im}\Pi^H(t)$,

$$a_\mu^{\text{QCD}} = \frac{4\alpha^2}{\pi} \int_{4m_\pi^2}^{\infty} \frac{1}{t} \text{Im}\Pi^H(t) K(t) dt. \quad (6)$$

We can relate (5) and (6) to QCD sum-rule methods by approximating Eq. (2) as

$$K(t) \approx \frac{m_\mu^2}{3t} = K_{\text{approx}}(t) \quad (7)$$

to obtain

$$a_\mu^{\text{QCD}} \approx \frac{4m_\mu^2\alpha^2}{3\pi} \int_{4m_\pi^2}^{\infty} \frac{1}{t^2} \text{Im}\Pi^H(t) dt, \quad (8)$$

where the effects of the approximation associated with (7) will be discussed below. The challenges of a QCD determination of $a_\mu^{\text{HVP,LO}}$ arise from the $1/t^2$ behaviour in (8) that emphasizes the low-energy region.

QCD sum-rules [10, 11] (see *e.g.*, [12–15] for reviews) implement quark-hadron duality by relating a QCD prediction to an integrated hadronic spectral function, and hence (8) suggests the possibility of using QCD sum-rules for determining $a_\mu^{\text{HVP,LO}}$. In particular, the structure of (8) is such that it can be written in terms of a finite-energy QCD sum rule (FESR) defined by [16–19]

$$F_k(s_0) = \int_{t_0}^{s_0} \frac{1}{\pi} \text{Im}\Pi^H(t) t^k dt, \quad (9)$$

where k is an integer that indicates the weight of the sum-rule and t_0 is a physical threshold. In (9), the left-hand side is obtained from a QCD prediction, and hence the FESRs relate a QCD prediction to an integrated hadronic spectral function. Writing (8) in terms of (9) gives

$$a_\mu^{\text{QCD}} \approx \frac{4m_\mu^2\alpha^2}{3} F_{-2}(\infty) \geq \frac{4m_\mu^2\alpha^2}{3} F_{-2}(s_0). \quad (10)$$

In the last step of Eq. (10), positivity of the hadronic spectral function has been used to obtain a lower bound. As outlined below, the presence of the parameter s_0 allows optimization of our theoretical prediction. Unfortunately, determining a field-theoretical expression for $F_{-2}(s_0)$ requires knowledge of low-energy constants, and hence a direct theoretical prediction is not possible. Various QCD sum-rule approaches have been used to circumvent this issue (see *e.g.*, Refs. [8, 9, 20, 21]). In this paper we examine the fundamental properties of the field theoretical result (10) through the application of the Hölder, Cauchy-Schwarz, and related inequalities to obtain QCD lower and upper bounds on the LO hadronic vacuum polarization contribution to the anomalous magnetic moment of the muon $a_\mu^{\text{HVP,LO}}$.

In Section 2 the fundamental inequalities for lower and upper bounds are developed. Section 3 provides the necessary QCD expressions and input parameters for light-quark (u, d, s) contributions up to five-loop order in perturbation theory in the chiral limit, LO in light-quark mass corrections, next-to-leading order (NLO) in dimension-four QCD condensates, and to LO in dimension-six QCD condensates. Analysis methodology and results for $a_\mu^{\text{HVP,LO}}$ are presented in Section 4, and the Appendix updates the Laplace sum-rule bounds on $a_\mu^{\text{HVP,LO}}$ in Ref. [8] with current determinations of the necessary QCD input parameters, five-loop perturbative corrections, and NLO dimension-four condensate contributions.

2 QCD Finite-Energy Sum Rule Bounds on a_μ^{QCD}

2.1 Lower Bounds

Hölder inequalities have previously been developed for QCD Laplace [22] and Gaussian sum-rules [23], and their application can be used to constrain the region of sum-rule parameter space in the

study of hadronic systems (see *e.g.*, Refs. [22–27]). Extending this Hölder inequality methodology to FESRs allows us to establish fundamental bounds on the theoretically-undetermined FESR $F_{-2}(s_0)$, leading to a constraint on a_μ^{QCD} via (10).

The Hölder inequality is expressed generally as [28, 29]

$$\left| \int_{t_1}^{t_2} f(t) g(t) d\mu \right| \leq \left(\int_{t_1}^{t_2} |f(t)|^p d\mu \right)^{\frac{1}{p}} \left(\int_{t_1}^{t_2} |g(t)|^q d\mu \right)^{\frac{1}{q}}, \quad \frac{1}{p} + \frac{1}{q} = 1. \quad (11)$$

With careful choice of functions $f(t)$, $g(t)$, and using positivity of $\text{Im}\Pi^H(t)$ to define the measure $d\mu = \frac{1}{\pi} \text{Im}\Pi^H(t) dt$ our Hölder inequality becomes

$$\left| \int_{t_0}^{s_0} t^{\alpha+\beta} \frac{1}{\pi} \text{Im}\Pi^H(t) dt \right| \leq \left(\int_{t_0}^{s_0} |t^\alpha|^p \frac{1}{\pi} \text{Im}\Pi^H(t) dt \right)^{\frac{1}{p}} \left(\int_{t_0}^{s_0} |t^\beta|^q \frac{1}{\pi} \text{Im}\Pi^H(t) dt \right)^{\frac{1}{q}}. \quad (12)$$

Because the QCD quantity $F_k(s_0)$ in Eq. (9) must inherit the properties associated with the hadronic spectral function, Eq. (12) can be expressed in terms of the FESRs

$$F_{\alpha+\beta}(s_0) \leq [F_{\alpha p}(s_0)]^{\frac{1}{p}} [F_{\beta q}(s_0)]^{\frac{1}{q}} \rightarrow F_{\alpha+\beta}(s_0) \leq [F_{\alpha p}(s_0)]^{\frac{1}{p}} \left[F_{\frac{\beta p}{p-1}}(s_0) \right]^{\frac{p-1}{p}}. \quad (13)$$

Eq. (13) results in a family of inequalities which can be used to place a lower bound on $F_{-2}(s_0)$. These are restricted due to the conditions from the Hölder inequality [Eq. (11)], as well due to the requirement from FESRs $F_k(s_0)$ that the weight k be an integer. By restricting our attention to inequalities that give a lower bound on $F_{-2}(s_0)$ through a combination of positive-weight FESR expressions, we derive the following inequalities:

$$F_{-2} \geq \frac{F_0^2}{F_2}, \quad (14)$$

$$F_{-2} \geq \frac{F_0^3}{F_1^2}, \quad (15)$$

$$F_{-2} \geq \frac{F_1^4}{F_2^3}, \quad (16)$$

where we have suppressed the s_0 dependence in each FESR. These inequalities place a lower bound on $F_{-2}(s_0)$ through a combination of FESRs that have weights low enough ($0 \leq k \leq 2$) to avoid dependence on unknown higher dimension QCD condensates as outlined below.

Having determined the lower bounds (14)–(16), we next determine which is the strongest restriction on F_{-2} . Starting from Eq. (13), we apply the substitutions $\alpha = \frac{k+1}{2}$ and $\beta = \frac{k-1}{2}$, and consider the Cauchy-Schwarz inequality (*i.e.*, the Hölder inequality in Eq. (13) with $p = q = 2$). This gives

$$F_k \leq F_{k+1}^{1/2} F_{k-1}^{1/2} \rightarrow F_k^2 \leq F_{k+1} F_{k-1}. \quad (17)$$

Rearranging this gives us a relationship between ratios of FESRs,

$$\frac{F_k}{F_{k+1}} \leq \frac{F_{k-1}}{F_k}. \quad (18)$$

Applying this to our constraints (14)–(16), we find the following hierarchy,

$$F_{-2} \geq \frac{F_0^3}{F_1^2} \geq \frac{F_0^2}{F_2} \geq \frac{F_1^4}{F_2^3}. \quad (19)$$

The most restrictive lower bound on $F_{-2}(s_0)$ is therefore provided by

$$F_{-2} \geq \frac{F_0^3}{F_1^2}. \quad (20)$$

From this, taking Eqs. (10) and (20), we can relate this inequality to a bound on a_μ^{QCD} ,

$$a_\mu^{\text{QCD}} \geq \frac{4m_\mu^2 \alpha^2}{3} \frac{F_0^3(s_0)}{F_1^2(s_0)}. \quad (21)$$

In obtaining the lower bound (21) on a_μ^{QCD} , the approximation in Eq. (7) has been used. The resulting lower bound (21) is only valid if this approximation is also a lower bound on $K(t)$. However, the approximation (7) provides an upper bound on $K(t)$, and $K_{\text{approx}}(t)$ must therefore be re-scaled by a factor ξ to obtain a valid lower bound

$$K_\xi(t) = \xi K_{\text{approx}}(t) = \xi \frac{m_\mu^2}{3t}. \quad (22)$$

The crucial energy region for determining ξ is the low-energy region from threshold to the ρ, ω peak. A naive Breit-Wigner σ^{BW} for the ρ, ω is non-zero at threshold and provides an overestimate of $\sigma^H(t)$ in the low-energy region. Thus ξ can be determined by the constraint

$$\int_{4m_\pi^2}^{m_\rho^2} K(t) \sigma^{\text{BW}}(t) dt \geq \int_{4m_\pi^2}^{m_\rho^2} K_\xi(t) \sigma^{\text{BW}}(t) dt. \quad (23)$$

The inequality (23) is saturated by $\xi = 0.83$, and as shown in Fig. 1, this value of ξ also results in a lower bound $K_\xi(t) \leq K(t)$ beyond the ρ, ω peak,

$$\int_{4m_\pi^2}^{\infty} K(t) \sigma^H(t) dt \geq \int_{4m_\pi^2}^{\infty} K_\xi(t) \sigma^H(t) dt. \quad (24)$$

Hence (21) is modified to our final form

$$a_\mu^{\text{QCD}} \geq \xi \frac{4m_\mu^2 \alpha^2}{3} \frac{F_0^3(s_0)}{F_1^2(s_0)}, \quad \xi = 0.83. \quad (25)$$

It should be noted from Fig. 1 that the approximate form $K_\xi(t)$ clearly underestimates the exact $K(t)$ above the ρ, ω peak, and hence the final bound in Eq. (25) is expected to be a conservative lower bound. Finally, the utility of the parameter s_0 appearing in (25) is now evident, because it can be varied to find the strongest possible QCD bound.

2.2 Upper Bounds

Because the kernel $K(t)$ decreases monotonically with increasing energy and $K(t) < K_{\text{approx}}(t)$ (see Fig. 1), the following upper bound can be obtained from (6) and (8)

$$a_\mu^{\text{QCD}} \leq \frac{4m_\mu^2 \alpha^2}{3\pi} \int_{t_0}^{\infty} \frac{1}{t^2} \text{Im}\Pi^H(t) dt \leq \frac{4m_\mu^2 \alpha^2}{3\pi} \frac{1}{t_0^2} \int_{t_0}^{\infty} \text{Im}\Pi^H(t) dt, \quad t_0 = 4m_\pi^2. \quad (26)$$

However, this bound can be improved by adapting and extending the techniques outlined in Ref. [30]. Ultimately, the goal is to construct an upper bound on $F_{-2}(s_0)$, but we illustrate the method of

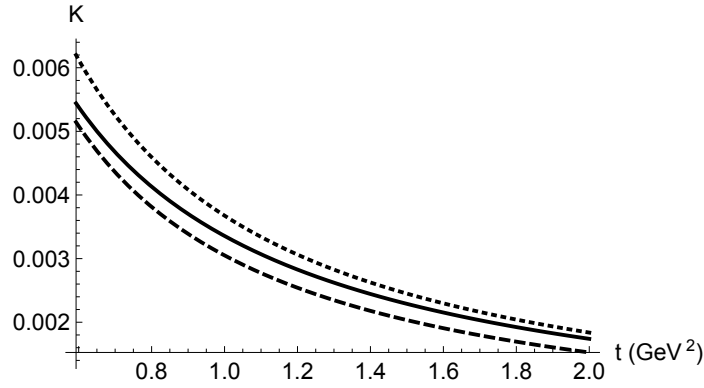


Figure 1: The exact $K(t)$ (solid line) compared to the approximate form $K_\xi(t)$ with $\xi = 0.83$ (lower dashed line) and with $\xi = 1$ (upper dotted line).

Ref. [30] with the necessary step of an upper bound on $F_{-1}(s_0)$ via the following relation based on positivity of the hadronic spectral function

$$\int_{t_0}^{s_0} \frac{1}{t} [1 + At]^2 \text{Im}\Pi^H(t) dt \geq 0. \quad (27)$$

By extremizing A to obtain the most stringent relation we find

$$F_{-1} \leq F_{-1}^{(B)} = \frac{F_0}{t_0} - \frac{(F_1/t_0 - F_0)^2}{(F_2/t_0 - F_1)}, \quad (28)$$

$$F_2/t_0 - F_1 > 0, \quad (29)$$

where the FESR dependence on s_0 has been suppressed and the subsidiary condition (29) is required for the validity of (28).

An upper bound on F_{-2} can then be obtained by extremizing the relation

$$\int_{t_0}^{s_0} \frac{1}{t^2} [1 + At]^2 \text{Im}\Pi^H(t) dt \leq \frac{1}{t_0} \int_{t_0}^{s_0} \frac{1}{t} [1 + At]^2 \text{Im}\Pi^H(t) dt, \quad (30)$$

to find

$$F_{-2} \leq \frac{F_{-1}^{(B)}}{t_0} - \frac{\left(F_0/t_0 - F_{-1}^{(B)}\right)^2}{(F_1/t_0 - F_0)}, \quad (31)$$

$$F_1/t_0 - F_0 > 0, \left(F_0/t_0 - F_{-1}^{(B)}\right)^2 < (F_0/t_0 - F_0^2/F_1)^2, \quad (32)$$

where the inequality $F_{-1} \geq F_0^2/F_1$ [see (17)] has been used as part of the subsidiary condition (32) for the validity of (31). An alternative upper bound on F_{-2} can be obtained by extremizing

$$\int_{t_0}^{s_0} \frac{1}{t^2} [1 + At]^2 \text{Im}\Pi^H(t) dt \leq \frac{1}{t_0^2} \int_{t_0}^{s_0} [1 + At]^2 \text{Im}\Pi^H(t) dt \quad (33)$$

to obtain

$$F_{-2} \leq F_0/t_0^2 - \frac{\left(F_1/t_0^2 - F_{-1}^{(B)}\right)^2}{(F_2/t_0^2 - F_0)}, \quad (34)$$

$$F_2/t_0^2 - F_0 > 0, \left(F_1/t_0^2 - F_{-1}^{(B)}\right)^2 < (F_1/t_0^2 - F_0^2/F_1)^2, \quad (35)$$

where the inequality $F_{-1} \geq F_0^2/F_1$ [see (17)] has again been used as part of the subsidiary condition (35) for the validity of (34).

Thus the upper QCD bound that is complimentary to the lower bound (21) is

$$a_\mu^{\text{QCD}} \leq \frac{4m_\mu^2\alpha^2}{3} \begin{cases} F_{-1}^{(B)}/t_0 - \frac{(F_0/t_0 - F_{-1}^{(B)})^2}{F_1/t_0 - F_0} \\ F_0/t_0^2 - \frac{(F_1/t_0^2 - F_{-1}^{(B)})^2}{F_2/t_0^2 - F_0} \end{cases}, \quad (36)$$

where either (31) or (34) is used for a QCD upper bound on F_{-2} . Both forms lead to identical numerical values despite the distinct pathways used to obtain them. Note that similar to the lower bound on F_{-2} in (20), the F_{-2} upper bounds (31) and (34) all depend on the well-determined QCD FESRs $\{F_0, F_1, F_2\}$, and similarly the parameter s_0 can be varied to find the strongest possible QCD bound. Combining (25) and (36), our a_μ^{QCD} bounds emerging from fundamental QCD sum-rule inequalities are

$$\xi \frac{4m_\mu^2\alpha^2}{3} \frac{F_0^3(s_0)}{F_1^2(s_0)} \leq a_\mu^{\text{QCD}} \leq \frac{4m_\mu^2\alpha^2}{3} \begin{cases} F_{-1}^{(B)}/t_0 - \frac{(F_0/t_0 - F_{-1}^{(B)})^2}{F_1/t_0 - F_0} \\ F_0/t_0^2 - \frac{(F_1/t_0^2 - F_{-1}^{(B)})^2}{F_2/t_0^2 - F_0} \end{cases}, \quad \xi = 0.83, \quad (37)$$

where the parameter s_0 can be varied independently on both sides of the inequality to find the strongest possible bounds.

3 Finite-Energy Sum-Rules: QCD Inputs

To generate a bound on a_μ^{QCD} from the FESRs in Eq. (37), correlation functions for the light quark vector current $j_\mu(x) = \bar{q}(x)\gamma_\mu q(x)$ provide the QCD prediction related to the hadronic spectral function in (9). The original LO calculation of the QCD correlation function $\Pi(Q^2)$ up to dimension-six in the operator-product expansion [10, 11, 31] (see also Refs. [8, 12, 13, 32]) has been extended to NLO in the dimension-four QCD condensates [26, 33, 34] and $\overline{\text{MS}}$ -scheme perturbative contributions up to five loop order in the chiral limit [35–41] (see also Refs. [42, 43])

$$\begin{aligned} \Pi(Q^2) = & \frac{1}{4\pi^2} \Pi^{\text{pert}}(Q^2) - \frac{3m_q^2(\nu)}{2\pi^2 Q^2} + 2\langle m_q \bar{q}q \rangle \frac{1}{Q^4} \left(1 + \frac{1}{3} \frac{\alpha_s(\nu)}{\pi}\right) \\ & + \frac{1}{12\pi} \langle \alpha_s G^2 \rangle \frac{1}{Q^4} \left(1 + \frac{7}{6} \frac{\alpha_s(\nu)}{\pi}\right) - \frac{224}{81} \pi \alpha_s \langle \bar{q}q q \bar{q} \rangle \frac{1}{Q^6}. \end{aligned} \quad (38)$$

In addition, $\Pi(Q^2)$ also requires an additional pre-factor of the quark charge Q_q^2 . The perturbative contributions in (38) are given by

$$\frac{1}{\pi} \text{Im} \Pi^{\text{pert}}(t, \nu) = S[x(\nu), L(\nu)] = 1 + \sum_{n=1}^{\infty} x^n \sum_{m=0}^{n-1} T_{n,m} L^m, \quad (39)$$

$$x(\nu) \equiv \frac{\alpha_s(\nu)}{\pi}, \quad L(\nu) \equiv \log\left(\frac{\nu^2}{t}\right), \quad (40)$$

where the coefficients $T_{n,m}$ given in Table 1 are implicitly a function of N_f , the number of active quark flavours. As outlined below, the energy range in our analysis results in a renormalization scale appropriate to $N_f = 3$ and $N_f = 4$. The QCD parameters necessary for Eqs. (9) and (38) are listed in Table 2.

$N_f = 4$	$m = 0$	$m = 1$	$m = 2$	$m = 3$	$N_f = 3$	$m = 0$	$m = 1$	$m = 2$	$m = 3$
$n = 1$	1	–	–	–	$n = 1$	1	–	–	–
$n = 2$	1.52453	25/12	–	–	$n = 2$	1.63982	9/4	–	–
$n = 3$	-11.6856	9.56054	625/144	–	$n = 3$	-10.2839	11.3792	81/16	–
$n = 4$	-92.91	-56.90	36.56	$\frac{15625}{1728}$	$n = 4$	-106.896	-46.2379	47.4048	729/64

Table 1: $\overline{\text{MS}}$ -scheme coefficients $T_{n,m}$ within (39) for the imaginary part of the vector-current correlation function up to five-loop order for $N_f = 4$ (left) and $N_f = 3$ (right). The four-loop results are given in Ref. [42], the five-loop coefficient $T_{4,0}$ is from [35], and five-loop logarithmic coefficients $T_{4,1}$, $T_{4,2}$, and $T_{4,3}$ are generated from the renormalization group analysis of Ref. [42] via the four-loop ($N_f = 4$ and $N_f = 3$) $\overline{\text{MS}}$ -scheme β function [44].

The FESR defined via (9) are now constructed up to five-loop order in perturbation theory in the chiral limit, LO in light-quark mass corrections, next-to-leading order (NLO) in dimension-four QCD condensates, and to LO in dimension-six QCD condensates. Using standard FESR methodology [16–19], the resulting FESR F_k for weights $k = \{0, 1, 2\}$ as needed for analysis of (19), (31), and (34) are given by

$$F_0(s_0) = \frac{1}{4\pi^2} \left[1 + \frac{\alpha_s(\nu)}{\pi} T_{1,0} + \left(\frac{\alpha_s(\nu)}{\pi} \right)^2 (T_{2,0} + T_{2,1}) + \left(\frac{\alpha_s(\nu)}{\pi} \right)^3 (T_{3,0} + T_{3,1} + 2T_{3,2}) \right. \\ \left. + \left(\frac{\alpha_s(\nu)}{\pi} \right)^4 (T_{4,0} + T_{4,1} + 2T_{4,2} + 6T_{4,3}) \right] s_0 - \frac{3}{2\pi^2} m_q(\nu)^2, \quad (41)$$

$$F_1(s_0) = \frac{1}{8\pi^2} \left[1 + \frac{\alpha_s(\nu)}{\pi} T_{1,0} + \left(\frac{\alpha_s(\nu)}{\pi} \right)^2 \left(T_{2,0} + \frac{1}{2} T_{2,1} \right) + \left(\frac{\alpha_s(\nu)}{\pi} \right)^3 \left(T_{3,0} + \frac{1}{2} T_{3,1} + \frac{1}{2} T_{3,2} \right) \right. \\ \left. + \left(\frac{\alpha_s(\nu)}{\pi} \right)^4 \left(T_{4,0} + \frac{1}{2} T_{4,1} + \frac{1}{2} T_{4,2} + \frac{3}{4} T_{4,3} \right) \right] s_0^2 \\ - 2\langle m_q \bar{q}q \rangle \left(1 + \frac{1}{3} \frac{\alpha_s(\nu)}{\pi} \right) - \frac{1}{12\pi} \langle \alpha_s G^2 \rangle \left(1 + \frac{7}{6} \frac{\alpha_s(\nu)}{\pi} \right), \quad (42)$$

Parameter	Value	Source
α	$1/137.036$	[45]
$\alpha_s(M_\tau)$	0.312 ± 0.015	[45]
$m_u(2 \text{ GeV})$	$2.16^{+0.49}_{-0.26} \text{ MeV}$	[45]
$m_d(2 \text{ GeV})$	$4.67^{+0.48}_{-0.17} \text{ MeV}$	[45]
$m_s(2 \text{ GeV})$	$(0.0934^{+0.0086}_{-0.0034}) \text{ GeV}$	[45]
f_π	$(0.13056 \pm 0.00019) / \sqrt{2} \text{ GeV}$	[45]
$m_n \langle \bar{n}n \rangle$	$-\frac{1}{2} f_\pi^2 m_\pi^2$	[46]
$m_s \langle \bar{s}s \rangle$	$r_m r_c m_n \langle \bar{n}n \rangle$	[47]
$r_c \equiv \langle \bar{s}s \rangle / \langle \bar{n}n \rangle$	0.66 ± 0.10	[47]
$m_s/m_n = r_m$	$27.33^{+0.67}_{-0.77}$	[45]
$\langle \alpha G^2 \rangle$	$(0.0649 \pm 0.0035) \text{ GeV}^4$	[48]
κ	3.22 ± 0.5	[48]
$\alpha_s \langle \bar{n}n \rangle^2$	$\kappa (1.8 \times 10^{-4}) \text{ GeV}^6$	[47]
$\alpha_s \langle \bar{s}s \rangle^2$	$r_c^2 \alpha_s \langle \bar{n}n \rangle^2$	[47]

Table 2: QCD parameters and uncertainties used in our analysis. Here, $m_n = (m_u + m_d)/2$ and $\langle \bar{n}n \rangle = \langle \bar{u}u \rangle = \langle \bar{d}d \rangle$.

$$\begin{aligned}
F_2(s_0) = \frac{1}{12\pi^2} & \left[1 + \frac{\alpha_s(\nu)}{\pi} T_{1,0} + \left(\frac{\alpha_s(\nu)}{\pi} \right)^2 \left(T_{2,0} + \frac{1}{3} T_{2,1} \right) + \left(\frac{\alpha_s(\nu)}{\pi} \right)^3 \left(T_{3,0} + \frac{1}{3} T_{3,1} + \frac{2}{9} T_{3,2} \right) \right. \\
& \left. + \left(\frac{\alpha_s(\nu)}{\pi} \right)^4 \left(T_{4,0} + \frac{1}{3} T_{4,1} + \frac{2}{9} T_{4,2} + \frac{2}{9} T_{4,3} \right) \right] s_0^3 - \frac{224}{81} \pi \alpha_s \langle \bar{q}q \bar{q}q \rangle. \quad (43)
\end{aligned}$$

Implicit in Eqs. (41)–(43) is a renormalization scale of $\nu = \sqrt{s_0}$ in both α_s and the running quark masses (see *e.g.*, Refs. [16–19]). This can be understood as arising from the renormalization-group equation satisfied by (39)

$$\left(-t \frac{\partial}{\partial t} + \beta(\alpha_s) \frac{\partial}{\partial \alpha_s} \right) \text{Im} \Pi^{\text{pert}}(t, \nu) = 0, \quad (44)$$

where the canonical and anomalous mass dimensions are zero for the vector current. From (44) it follows that the FESRs satisfy the following renormalization-group equation

$$\left(-s_0 \frac{\partial}{\partial s_0} + \beta(\alpha_s) \frac{\partial}{\partial \alpha_s} + (k+1) \right) F_k^{\text{pert}}(s_0, \nu) = 0, \quad (45)$$

$$F_k^{\text{pert}}(s_0, \nu) = \int_0^{s_0} t^k \frac{1}{\pi} \text{Im} \Pi^{\text{pert}}(t, \nu) dt. \quad (46)$$

Thus apart from the trivial s_0^{k+1} canonical dimension prefactor, the solution of the renormalization-group equation for the QCD expressions (41)–(43) is obtained by the standard replacement $\nu^2 = s_0$. For renormalization-group behaviour of the dimension-four NLO contributions, it is helpful to recall that $\langle m_q \bar{q}q \rangle$ and $\langle \beta G^2 \rangle + 4\gamma \langle m_q \bar{q}q \rangle$ are renormalization-group invariant (see *e.g.*, Ref. [32]).

In particular, because we are working to $\mathcal{O}(\alpha_s^4)$ in perturbation theory, we numerically solve the renormalization-group equation using the four-loop $\overline{\text{MS}}$ -scheme β function [44] with N_f appropriate to the active flavours below s_0 and using $\alpha_s(M_\tau)$ as a boundary condition. For the running quark mass corrections, only the LO ($\overline{\text{MS}}$ -scheme) anomalous mass dimension is needed. As outlined below, this s_0 energy region will span the range covered by $N_f = 4$ and $N_f = 3$. We do not implement flavour threshold matching conditions [49] (see *e.g.*, Ref. [50] for an example implementation) because such effects are insignificant compared to other sources of theoretical uncertainty. Finally, the generic light-flavour FESRs (41)–(43) require a pre-factor of their quark charge (*i.e.*, $Q_u^2 = 4/9$ and $Q_d^2 = Q_s^2 = 1/9$).

4 Analysis Methodology and Results

With the FESRs now defined in Eqs. (41)–(43), a lower bound on a_μ^{QCD} can be constructed via (25) [see also (37)]. The methodology seeks to optimize s_0 such that it simultaneously maximizes the ratio F_0^3/F_1^2 to obtain the strongest possible bound, while still satisfying the inequality (17) with $k = 1$. This ensures that the resulting s_0^{opt} is in the region of validity for the FESRs because they satisfy the same inequality properties as an integrated hadronic spectral function. We start scanning s_0 from large energy (beginning near bottom threshold in $N_f = 4$ regime) and find that stronger bounds trend toward lower s_0 . We then transition to $N_f = 3$ below the charm threshold (uncertainties associated with the Ref. [45] value for the $m_c(m_c) = 1.27 \text{ GeV}$ threshold are negligible).

We use two different implementations of this optimization methodology. The flavour-separated approach applies the methodology to the FESRs (with each charge factor included) for each flavour separately, and then combines the individual optimized flavour contributions to obtain the final bound on a_μ^{QCD} . In the flavour-combined approach, the methodology is applied to a combined FESR with a sum over flavours (with their charge factors included). The strongest bound from these two implementations is then used for our final prediction of the lower bound on a_μ^{QCD} .

We find that the flavour-separated approach leads to the strongest bound, and Table 3 shows the results for the central values of the QCD input parameters of Table 2. There are a few key points in the interpretation of Table 3. First, it is important to remember that (25) is truly a bound, and the optimized s_0^{opt} represents the value which maximizes the bound while simultaneously satisfying the $k = 1$ inequality (17). It is therefore incorrect to interpret s_0^{opt} as a cut-off on the QCD contributions. Second, the only field-theoretical distinction between the u and d contributions arises from the very small effect of quark masses, and hence s_0^{opt} is the same in the non-strange channels and the bounds on a_μ^{QCD} are in the ratio of quark charges $Q_u^2/Q_d^2 = 4$. Third, the strange contributions to the a_μ^{QCD} bound are roughly an order of magnitude smaller than non-strange, a feature that aligns with the data-driven and LQCD approaches to $a_\mu^{\text{HVP,LO}}$ [3, 51]. Finally, we note that the entire inequality analysis of Section 2 would also apply to Laplace sum-rules, leading to analogous expressions for Eq. (25). We have explored this possibility and find that the Laplace sum-rule bounds are considerably weaker than for FESRs, presumably because the Laplace sum-rule kernel $\exp(-t\tau)$ suppresses higher-energy contributions compared to the polynomial FESR kernels.

An uncertainty analysis was performed to determine the sensitivity of the Table 3 lower a_μ^{QCD} bounds arising from the QCD input parameters in Table 2. The uncertainty of the a_μ^{QCD} bound is dominated by changes in the vacuum saturation parameter κ and in the uncertainty of the dimension-four gluon condensate parameter $\langle\alpha G^2\rangle$ (the poorly known strange-quark condensate parameter r_c is a sub-dominant effect because the strange contributions in Table 3 are much smaller than non-strange). Taking into account the combined effect of these uncertainties gives our final QCD

Flavour	s_0^{opt} (GeV ²)	a_μ^{QCD} (lower bound)	a_μ^{QCD} (upper bound)
u	1.09	$\geq 472.7 \times 10^{-10}$	$\leq 567.2 \times 10^{-10}$
d	1.09	$\geq 118.1 \times 10^{-10}$	$\leq 141.7 \times 10^{-10}$
s	1.19	$\geq 66.2 \times 10^{-10}$	$\leq 79.5 \times 10^{-10}$
Total	–	$\geq 657.0 \times 10^{-10}$	$\leq 788.4 \times 10^{-10}$

Table 3: The optimized s_0^{opt} and corresponding bounds on a_μ^{QCD} are shown for each flavour in the flavour-separated method for central values of the QCD input parameters of Table 2. The total entry represents the sum of the individual flavour contributions for the final predicted bounds on a_μ^{QCD} .

prediction for the light-quark contributions lower bound

$$a_\mu^{\text{QCD}} \geq (657.0 \pm 34.8) \times 10^{-10}. \quad (47)$$

A similar methodology is used to analyze the upper bounds associated with Eq. (36) [see also (37)] using either (31) or (34) for the upper bound on F_{-2} . We seek the strongest bound that simultaneously satisfies the $k = 1$ inequality (17) along with the conditions (29), (32), and (35). As in the lower bound analysis, the flavour-separated approach leads to the strongest bound, and the same s_0^{opt} is obtained because the $k = 1$ Cauchy-Schwarz inequality (17) turns out to be a limiting constraint in both cases. The results shown in Table 3 along with the theoretical uncertainty gives our final QCD prediction for the light-quark contributions upper bound

$$a_\mu^{\text{QCD}} \leq (788.4 \pm 41.8) \times 10^{-10}. \quad (48)$$

For purposes of comparison with data-driven approaches, we first note that although we are calculating light-quark contributions (and ultimately using $N_f = 3$ virtual corrections in the final results), our determinations (47) and (48) still incorporate high-energy perturbative contributions to a_μ^{QCD} . We are thus underestimating the perturbative contributions above the charm threshold, and so our bounds remain valid. Thus we have to supplement our bounds with charmonium and bottomonium resonance contributions of $a_{\mu, \bar{c}c, \bar{b}b}^{\text{HVP,LO}} = (7.93 \pm 0.19) \times 10^{-10}$ from [51] to obtain our total bound for comparison purposes

$$(664.9 \pm 34.8) \times 10^{-10} \leq a_\mu^{\text{HVP,LO}} \leq (796.3 \pm 41.8) \times 10^{-10} \quad (49)$$

which should be compared with the data-driven Ref. [51] result

$$a_\mu^{\text{HVP,LO}} = (692.78 \pm 2.42) \times 10^{-10}, \quad (50)$$

the data-driven result reported in the $(g - 2)$ Theory Initiative Whitepaper [3]

$$a_\mu^{\text{HVP,LO}} = (693.1 \pm 4.0) \times 10^{-10}, \quad (51)$$

as well as the result from LQCD reported in the $(g - 2)$ Theory Initiative Whitepaper [3],

$$a_\mu^{\text{HVP,LO}} = (711.6 \pm 18.4) \times 10^{-10}. \quad (52)$$

These values can be seen compared against our bounds in Figure 2.

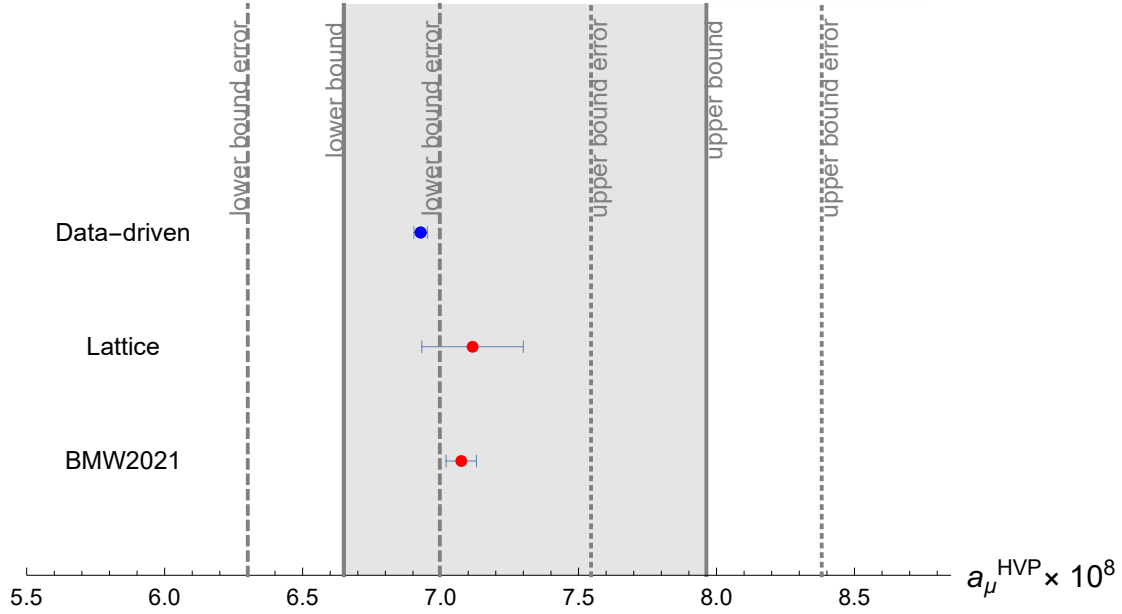


Figure 2: The a_μ^{QCD} results (49) showing lower bound (long dashed lines reflecting theoretical uncertainties) and upper bound (short dashed lines reflecting theoretical uncertainties) in comparison to the $a_\mu^{\text{HVP,LO}}$ world theoretical averages given in [3]. The blue indicates a data-driven methodology, while red indicates a value obtained via LQCD. Both the LQCD world average [3] and the sub-percent precision calculation from the BMW collaboration [5] are shown for comparison. The grey shaded region illustrates the allowed central-value range of our QCD predictions in Eq. (49).

In conclusion, we have constructed bounds on the QCD contributions to $a_\mu^{\text{HVP,LO}}$ using a family of Hölder inequalities and related inequality constraints for QCD finite-energy sum-rules (FESRs). These fundamental inequalities are based on the requirement that the QCD FESRs are consistent with the relation (9) to an integrated hadronic spectral function, providing a novel methodology complementary to lattice QCD and data-driven approaches to determining $a_\mu^{\text{HVP,LO}}$. Analyzing the light-quark (u, d, s) contributions up to five-loop order in perturbation theory in the chiral limit, LO in light-quark mass corrections, NLO in dimension-four QCD condensates, and to LO in dimension-six QCD condensates leads to our QCD bounds in Eqs. (47) and (48), which can be supplemented with the well-known contributions from charmonium and bottomonium states to obtain the QCD bounds given in Eq. (49). As shown in the Appendix, these FESR bounds are more restrictive than the updated Laplace sum-rule bounds using the approach of Ref. [8]. As illustrated in Fig. 2, the central values of our total QCD bounds (49) thus bridge the region between LQCD and data-driven values, indicating a possible resolution of the tension between LQCD and data-driven determinations of $a_\mu^{\text{HVP,LO}}$. Resolving this tension would provide better guidance to searches for new physics in measurements of the anomalous magnetic moment of the muon. In future work we will search for new methods and new fundamental inequalities to improve bounds on the QCD contributions to $a_\mu^{\text{HVP,LO}}$.

Acknowledgments

TGS is grateful for research funding from the Natural Sciences and Engineering Research Council of Canada (NSERC).

Appendix: Laplace Sum Rule Approach

QCD Laplace sum-rules [10,11] are similar to finite-energy sum-rules as defined in (9); however, they are constructed using a Borel (inverse Laplace) transform which introduces an exponential factor:

$$L_k(\tau, s_0) = \int_{t_0}^{s_0} \frac{1}{\pi} \text{Im}\Pi^H(t) t^k e^{-t\tau} dt. \quad (53)$$

In [8] it was shown that $a_\mu^{\text{HVP,LO}}$, as defined in (6), can be expressed as a linear combination of QCD Laplace sum-rules (53). First, the exact kernel function (2) can be approximated near $t = t'$ as

$$K(t) \approx \mathcal{K}(t, t') = K(t') e^\zeta \left[a_1 \left(\frac{t}{t'} \right) + a_2 \left(\frac{t}{t'} \right)^2 + a_3 \left(\frac{t}{t'} \right)^3 \right] e^{-\zeta t/t'}, \quad (54)$$

where $a_1 + a_2 + a_3 = 1$ so that $K(t') = \mathcal{K}(t', t')$. Inserting (54) into (6) yields

$$a_\mu^{\text{QCD}} \approx 4\alpha^2 K(t') \frac{e^\zeta}{t'} \int_{t_0}^{\infty} \frac{1}{\pi} \text{Im}\Pi^H(t) \left[a_1 + a_2 \left(\frac{t}{t'} \right) + a_3 \left(\frac{t}{t'} \right)^2 \right] e^{-\zeta t/t'} dt, \quad (55)$$

where $t_0 = 4m_\pi^2$. Introducing the parameter s_0 as in (10) and defining $\tau = \zeta/t'$, (55) becomes

$$a_\mu^{\text{QCD}} \approx 4\alpha^2 K(\zeta/\tau) \frac{\tau}{\zeta} e^\zeta \int_{t_0}^{s_0} \frac{1}{\pi} \text{Im}\Pi^H(t) \left[a_1 + a_2 \left(\frac{t}{t'} \right) + a_3 \left(\frac{t}{t'} \right)^2 \right] e^{-t\tau} dt. \quad (56)$$

Comparing (56) and the definition of the Laplace sum-rules in (53) shows that we may approximate $a_\mu^{\text{HVP,LO}}$ as a linear combination of Laplace sum-rules:

$$a_\mu^{\text{QCD}} \approx 4\alpha^2 K(\zeta/\tau) \frac{\tau}{\zeta} e^\zeta \left[a_1 L_0(\tau, s_0) + a_2 \frac{\tau}{\zeta} L_1(\tau, s_0) + a_3 \left(\frac{\tau}{\zeta} \right)^2 L_2(\tau, s_0) \right]. \quad (57)$$

The approximation (54) is used because it makes a theoretical calculation of $a_\mu^{\text{HVP,LO}}$ (using a QCD expression for the vacuum polarization function) amenable to a Laplace sum-rule analysis. In (54) the expansion is truncated at $\mathcal{O}(t^3)$ to avoid dependence on unknown higher dimension QCD condensates (a similar issue is encountered in the finite-energy sum-rule analysis in Section 2).

Although the approximation (54) is designed to be exact at $t = t'$ and is well suited to a Laplace sum-rule analysis, the approximation of the exact kernel function (2) decreases in accuracy away from $t = t'$. In order to gain some control over the theoretical uncertainty introduced by this approximation we will follow the approach of Ref. [8], wherein the approximation (54) was used to construct underestimates and overestimates of the exact kernel function (2), respectively denoted as $\mathcal{K}^\downarrow(t, t')$ (corresponding to parameters $\{a_1 = 1.5700, a_2 = -1.75658, a_3 = 1.1958, \zeta = 2.6528\}$) and $\mathcal{K}^\uparrow(t, t')$ (corresponding to parameters $\{a_1 = 6.0378, a_2 = -10.7006, a_3 = 5.6628, \zeta = 2.6528\}$), which are shown in Fig. 3. Using these underestimates and overestimates, a QCD Laplace sum-rule analysis can be performed to generate lower and upper bounds on $a_\mu^{\text{HVP,LO}}$.

Using the results of Eqs. (38) and (39), the Laplace sum-rules (LSRs) for light-quark (u, d, s) contributions up to five-loop order in perturbation theory in the chiral limit, LO in light-quark mass corrections, next-to-leading order (NLO) in dimension-four QCD condensates, and to LO in

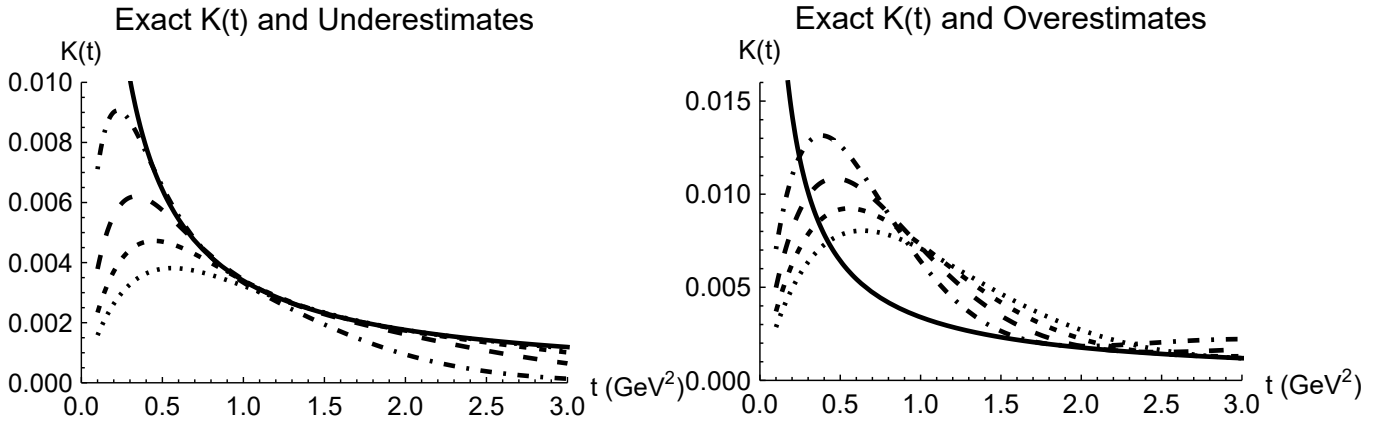


Figure 3: Left: the exact $K(t)$ (solid line) compared to underestimates $\mathcal{K}^\downarrow(t, t')$ with $t' \in \{0.8, 1.2, 1.6, 2.0\}$ GeV^2 , which are respectively represented by the dashed dotted, long dashed, short dashed, and dotted lines. Right: the exact $K(t)$ (solid line) compared to overestimates $\mathcal{K}^\uparrow(t, t')$ with $t' \in \{1.8, 2.2, 2.6, 3.0\}$ GeV^2 , which are respectively represented by dashed dotted, long dashed, short dashed, and dotted lines. The parameters used in equation (54) for the underestimates $\mathcal{K}^\downarrow(t, t')$ ($\{a_1 = 1.5700, a_2 = -1.75658, a_3 = 1.1958, \zeta = 2.6528\}$) and overestimates $\mathcal{K}^\uparrow(t, t')$ ($\{a_1 = 6.0378, a_2 = -10.7006, a_3 = 5.6628, \zeta = 2.6528\}$) are identical to those used in Ref. [8].

dimension-six QCD condensates are given for a generic light flavour by

$$L_0(\tau, s_0) = \frac{1}{4\pi^2\tau} \left[f_{0,0}(\tau s_0) + \sum_{k=0}^3 f_{0,k}(\tau s_0) \sum_{j=k+1}^4 T_{j,k} \left(\frac{\alpha_s(\nu)}{\pi} \right)^j \right] - \frac{3}{2\pi^2} m_q(\nu)^2 + 2\langle m_q \bar{q}q \rangle \left(1 + \frac{1}{3} \frac{\alpha_s(\nu)}{\pi} \right) \tau + \frac{1}{12\pi} \langle \alpha_s G^2 \rangle \left(1 + \frac{7}{6} \frac{\alpha_s(\nu)}{\pi} \right) \tau - \frac{112}{81} \pi \alpha_s \langle \bar{q}q \bar{q}q \rangle \tau^2, \quad (58)$$

$$L_1(\tau, s_0) = \frac{1}{4\pi^2\tau^2} \left[f_{1,0}(\tau s_0) + \sum_{k=0}^3 f_{1,k}(\tau s_0) \sum_{j=k+1}^4 T_{j,k} \left(\frac{\alpha_s(\nu)}{\pi} \right)^j \right] - 2\langle m_q \bar{q}q \rangle \left(1 + \frac{1}{3} \frac{\alpha_s(\nu)}{\pi} \right) - \frac{1}{12\pi} \langle \alpha_s G^2 \rangle \left(1 + \frac{7}{6} \frac{\alpha_s(\nu)}{\pi} \right) + \frac{224}{81} \pi \alpha_s \langle \bar{q}q \bar{q}q \rangle \tau, \quad (59)$$

$$L_2(\tau, s_0) = \frac{1}{4\pi^2\tau^3} \left[f_{2,0}(\tau s_0) + \sum_{k=0}^3 f_{2,k}(\tau s_0) \sum_{j=k+1}^4 T_{j,k} \left(\frac{\alpha_s(\nu)}{\pi} \right)^j \right] - \frac{224}{81} \pi \alpha_s \langle \bar{q}q \bar{q}q \rangle, \quad (60)$$

where we have defined the quantity

$$f_{j,k}(\tau s_0) = \int_0^{\tau s_0} z^j \left[\log \left(\frac{1}{z} \right) \right]^k e^{-z} dz. \quad (61)$$

Implicit in Eqs. (58)–(60) is a renormalization scale of $\nu = 1/\sqrt{\tau}$ in both α_s and the running quark masses [52]. As in the QCD expressions (41)–(43) for the FESRs, the generic light-flavour LSRs (58)–(60) require a pre-factor of their quark charge.

Following the analysis methodology Ref. [8] for determining the upper and lower bounds on a_μ^{QCD} , τ stability [53–55] is used to determine the right-hand side of (57) for a fixed s_0 , and then s_0 is varied until an asymptotic value is reached. The τ -stability region naturally tends toward the $N_f = 3$ regime. As with the FESRs, this methodology can be applied to either a flavour-separated

or flavour-combined case, but unlike the FESRs there is negligible difference in the two cases. Fig. 4 shows the results for central values of the QCD input parameters, and leads to the bounds

$$369.5 \times 10^{-10} \leq a_\mu^{\text{QCD}} \leq 930.2 \times 10^{-10}. \quad (62)$$

Comparing Eq. (62) with the FESR results in Eqs. (47) and (48) it is evident that the FESR bounds are stronger than those obtained from updated and extended QCD inputs in the Ref. [8] LSR methodology.

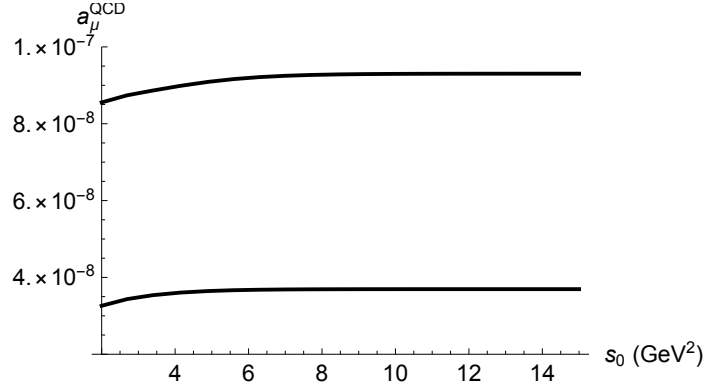


Figure 4: LSR upper bound (top curve) and lower bound (bottom curve) on light-quark contributions to a_μ^{QCD} as a function of s_0 .

References

- [1] The Muon $g - 2$ Collaboration, D. P. Aguillard et al., Phys. Rev. Lett. **131**, 161802 (2023).
- [2] D. P. Aguillard et al., (2024), [arXiv:2402.15410 [hep-ex]].
- [3] T. Aoyama et al., Physics Reports **887**, 1 (2020).
- [4] CMD-3, F. V. Ignatov et al., Phys. Rev. Lett. **132**, 231903 (2024), 2309.12910.
- [5] S. Borsanyi et al., Nature **593**, 51 (2021), [arXiv:2002.12347 [hep-lat]].
- [6] S. Kuberski, PoS **LATTICE2023**, 125 (2024), [arXiv:2312.13753 [hep-lat]].
- [7] B. E. Lautrup and E. de Rafael, Phys. Rev. **174**, 1835 (1968).
- [8] T. G. Steele, N. C. A. Hill, V. Elias, and R. B. Mann, Phys. Rev. D **44**, 3610 (1991).
- [9] I. Caprini, J. Cole, and C. Verzegnassi, Nuovo Cim. A **83**, 121 (1984).
- [10] M. A. Shifman, A. I. Vainshtein, and V. I. Zakharov, Nucl. Phys. **B147**, 385 (1979).
- [11] M. A. Shifman, A. I. Vainshtein, and V. I. Zakharov, Nucl. Phys. **B147**, 448 (1979).
- [12] L. J. Reinders, H. Rubinstein, and S. Yazaki, Phys. Rept. **127**, 1 (1985).
- [13] S. Narison, QCD as a Theory of Hadrons : From Partons to Confinement, Camb. Monogr. Part. Phys. Nucl. Phys. Cosmol. Vol. 17 (Oxford University Press, 2005), [arXiv:hep-ph/0205006].

- [14] P. Gubler and D. Satow, *Prog. Part. Nucl. Phys.* **106**, 1 (2019).
- [15] P. Colangelo and A. Khodjamirian, QCD sum rules, a modern perspective, in *At The Frontier of Particle Physics*, edited by M. Shifman and B. Ioffe, pp. 1495–1576, 2000, [arXiv:hep-ph/0010175].
- [16] E. G. Floratos, S. Narison, and E. de Rafael, *Nucl. Phys. B* **155**, 115 (1979).
- [17] W. Hubschmid and S. Mallik, *Nucl. Phys. B* **193**, 368 (1981).
- [18] R. A. Bertlmann, G. Launer, and E. de Rafael, *Nucl. Phys. B* **250**, 61 (1985).
- [19] I. Caprini and C. Verzegnassi, *Nuovo Cim. A* **90**, 388 (1985).
- [20] J. A. Casas, C. Lopez, and F. J. Yndurain, *Phys. Rev. D* **32**, 736 (1985).
- [21] S. Narison, *Nucl. Phys. A* **1039**, 122744 (2023), [arXiv:2306.14639 [hep-ph]].
- [22] M. Benmerrouche, G. Orlandini, and T. G. Steele, *Phys. Lett. B* **356**, 573 (1995), [arXiv:hep-ph/9507304].
- [23] J. Ho, R. Berg, W. Chen, D. Harnett, and T. G. Steele, *Phys. Rev. D* **98**, 096020 (2018), [arXiv:1806.02465 [hep-ph]].
- [24] T. G. Steele, K. Kostuik, and J. Kwan, *Phys. Lett. B* **451**, 201 (1999), [arXiv:hep-ph/9812497].
- [25] F. Shi *et al.*, *Nucl. Phys. A* **671**, 416 (2000), [arXiv:hep-ph/9909475].
- [26] Q.-N. Wang, Z.-F. Zhang, T. G. Steele, H.-Y. Jin, and Z.-R. Huang, *Chin. Phys. C* **41**, 074107 (2017), [arXiv:1612.00808 [hep-ph]].
- [27] J.-M. Yuan, Z.-F. Zhang, T. G. Steele, H.-Y. Jin, and Z.-R. Huang, *Phys. Rev. D* **96**, 014034 (2017), [arXiv:1705.00397 [hep-ph]].
- [28] E. F. Beckenbach and R. Bellman, *Inequalities* (Springer, Berlin, 1961).
- [29] S. K. Berberian, *Measure and Integration* (MacMillan, New York, 1965).
- [30] F. Dalfovo and S. Stringari, *Phys. Rev. B* **46**, 3991 (1992), [arXiv:cond-mat/9210021].
- [31] L. J. Reinders and H. R. Rubinstein, *Phys. Lett. B* **145**, 108 (1984).
- [32] P. Pascual and R. Tarrach, *QCD: Renormalization for the Practitioner*, Lecture Notes in Physics Vol. 194 (Springer, Berlin, Heidelberg, 1984).
- [33] L. R. Surguladze and F. V. Tkachov, *Nucl. Phys. B* **331**, 35 (1990).
- [34] K. G. Chetyrkin, V. P. Spiridonov, and S. G. Gorishnii, *Phys. Lett. B* **160**, 149 (1985).
- [35] P. A. Baikov, K. G. Chetyrkin, and J. H. Kühn, *Phys. Rev. Lett.* **101**, 012002 (2008).
- [36] S. G. Gorishnii, A. L. Kataev, and S. A. Larin, *Phys. Lett. B* **259**, 144 (1991).
- [37] L. R. Surguladze and M. A. Samuel, *Phys. Rev. Lett.* **66**, 560 (1991), [Erratum: *Phys. Rev. Lett.* **66**, 2416 (1991)].

- [38] K. G. Chetyrkin, Phys. Lett. B **391**, 402 (1997), [arXiv:hep-ph/9608480].
- [39] K. G. Chetyrkin, A. L. Kataev, and F. V. Tkachov, Phys. Lett. B **85**, 277 (1979).
- [40] M. Dine and J. R. Sapiirstein, Phys. Rev. Lett. **43**, 668 (1979).
- [41] W. Celmaster and R. J. Gonsalves, Phys. Rev. Lett. **44**, 560 (1980).
- [42] M. R. Ahmady et al., Phys. Rev. D **67**, 034017 (2003).
- [43] D. d’Enterria et al., (2022), [arXiv:2203.08271 [hep-ph]].
- [44] T. van Ritbergen, J. A. M. Vermaseren, and S. A. Larin, Phys. Lett. B **400**, 379 (1997), [arXiv:hep-ph/9701390].
- [45] Particle Data Group, R. L. Workman et al., PTEP **2022**, 083C01 (2022).
- [46] M. Gell-Mann, R. J. Oakes, and B. Renner, Phys. Rev. **175**, 2195 (1968).
- [47] D. Harnett, J. Ho, and T. G. Steele, Phys. Rev. D **103**, 114005 (2021), [arXiv:2104.00752v4 [hep-ph]].
- [48] R. Albuquerque, S. Narison, and D. Rabetiarivony, Nucl. Phys. A **1039**, 122743 (2023), [arXiv:2305.02421 [hep-ph]].
- [49] K. G. Chetyrkin, B. A. Kniehl, and M. Steinhauser, Nucl. Phys. B **510**, 61 (1998), hep-ph/9708255.
- [50] T. G. Steele and V. Elias, Mod. Phys. Lett. A **13**, 3151 (1998), hep-ph/9902217.
- [51] A. Keshavarzi, D. Nomura, and T. Teubner, Phys. Rev. D **101**, 014029 (2020).
- [52] S. Narison and E. de Rafael, Phys. Lett. B **103**, 57 (1981).
- [53] J. S. Bell and R. Bertlmann, Nucl. Phys. B **177**, 218 (1981).
- [54] J. S. Bell and R. A. Bertlmann, Nucl. Phys. B **187**, 285 (1981).
- [55] S. Narison, (2023), [arXiv:2309.00258 [hep-ph]].